4-C seismic data processing experience in Brazil

Mércia B. C. e Silva, GTEP/PUC-Rio; Odilon Keller Filho, PETROBRAS; Marcos A. G. Guimarães, PETROBRAS; Rob Windels, Fairfield Industries Inc.; Ricardo Leiderman, GTEP/PUC-Rio; Fredy A. V. Artola, GTEP/PUC-Rio; Sérgio A. B. da Fontoura, GTEP/PUC-Rio; Jorge F. F. Sobreira, PETROBRAS

Abstract

Two 2D/4C seismic lines were acquired experimentally, using ocean bottom cable (OBC), in transition zone (water depth<10m) at Serra Field, Potiguar Basin, Northern Brazil. Two sensors – one geophone and one hydrophone – were used to record PP-wave. The other two sensors, radial and transversal geophones, were used to record converted wave (PS). The final P-wave section, with dual sensor summing (hydrophone + vertical geophone), shows better image than the one obtained processing only the data from the hydrophone. The best processing technique for converted wave was pre-stack time migration. The converted wave section (radial geophone) shows similar image quality as P-wave section for vertical geophone.

Introduction

S-wave information can be acquired directly from special seismic surveys. Onshore, the S-wave may be either generated by special vibrators and recorded by three component geophones (3C) or recorded as PS conversion at seismic reflectors.

Offshore, the S-wave is, in general, generated as converted waves and recorded as such at the ocean bottom since air gun arrays generate only pressure wave-field. Two horizontal geophones are placed at the ocean bottom and connected by cabling to the recording equipment. The PS mode means down-going field being P-wave and up-coming wave-field being S-wave. Other conversions through the interfaces are not considered in this paper. A velocity field sensor, vertical geophone, and a pressure field device, hydrophone, record the P-wave. The converted wave is recorded by two horizontal geophones (radial and transversal). Therefore, each receiver station has four components (4C) (Stewart *et al*., 2002).

The reason to record the P-wave using two components is to eliminate the ghost effect generated at free surface (Hoffe *et al*. 1999). The ghost effect interference depends on the water depth. For depths less than 10m, the ghost effect does not affect the seismic bandwidth. Therefore, various transition zones OBC crews use only one hydrophone in the receiver station.

Grant Geophysical/Petrobras, in 2001, acquired two experimental 4C lines in transition zone with water depth below 10m at the Serra field in Potiguar Basin. The study of these lines was part of a large research project named Acquisition Geometry of Multicomponent Seismic Data, carried out by the Laboratory of Computational Geosciences of PUC Rio, (LCG/GTEP/PUC-Rio), through a research cooperation agreement with Petrobras. Additionally, this project had the participation of Fairfield Industries Inc. that kindly provided the results of a 4C experimental line acquired in Gulf of Mexico and acted as consultants for the seismic processing activities. In this paper, we present part of the data processing carried out with one of these 4C lines in order to obtain the final PP and PS-wave images and to define a good processing sequence.

The software for seismic processing used some conventional techniques for P- and S-waves and some techniques built for converted waves. Numerical seismic modeling was used to compute conversion point's position for the main geological events and to validate CCP fold for this acquisition.

Data acquisition and geometry

The dataset corresponds to two 2D/4C lines acquired in transition zone, with a water depth between 2m and 8m (Neill *et al.* 2001). Due to the lack of sensor availability, the acquisition was made using only 24 4-C receivers. These receivers were spread along three lines, followed one by one in order to build a final acquisition line with 72 receivers crossing the area to be investigated. The shot line length was approximately 9.5km. The shot and receiver lines are in the same direction (Fig.1).

The seismic sources used were an array of GI air guns (Sodera). The gun depth operation was 3m. For each entire receiver line (24 receivers), two shot lines were shot at the same position staggered by 12,5m (Fig.1).

The acquisition cables were tensioned, after deployment, as an attempt to assure that the radial sensor is aligned with the receiver line. Therefore, no vector fidelity was needed. Analogical-digital converter boxes with eight channels were used during acquisition, *i.e.*, two 4C receivers/box. These 4C receivers were connected as depicted in Figure 2. Besides, the wave-field generated by shots in each side of the radial geophone was recorded with different polarities. Thus, it was necessary to organize the data associated to each component and to correct polarity according to shot position (Fig.3).

Converted wave processing

The PS-wave processing was carried out with ProGOLD® software (Fairfield's proprietary computer code) running as ProMAX® add-in. Several converted wave processing-algorithms are included in the software. The main sequence applied to the lines was based on Harrison, (1992). Figure 4 depicts the main steps of the processing flow. They are briefly described next.

Noise removal and deconvolution

Multi-channel and time-varying band pass filters were applied to the data to remove mud-roll and other low velocity events. Shallow water guided waves were removed using FK filter. A zero-phase deconvolution (time-varying spectral whitening) was applied to the data to enhance the vertical resolution.

Velocity analysis

Conventional programs to NMO correct CCP gathers were used. Due to the nonsymmetrical trajectory of the PS rays (non-hyperbolic) and due to the low quality of the data, moveout analysis for Serra data resulted in mapping different conversion events (probably PSS or other complex modes). Seismic modeling studies, carried out for comparisons with the seismic data, showed that the velocity picked for data analysis was slower than expected PS-wave RMS velocity.

This difference between picked and modeled velocity is caused by approximations when evaluating conversion points. The common conversion points (CCP) are different from the P-wave common mid point (CMP). Therefore, special technique that requires the Vp/Vs ratio was used to compute the position of these points. The initial value used was a constant Vp/Vs=1.8, obtained from well log information. A more accurate Vp/Vs ratio was obtained from the seismic data processing

Conversion point

The technique to process P-wave data uses trace gathers at CMP location (source-receiver common mid point). Laterally low velocity variation causes the P-wave reflection to occur at CMP location (Yilmaz, 1997). On the other hand, CCP (common conversion point) never falls on CMPs. It varies with depth of the reflector and formation properties.

The algorithm used to sort the CCP traces in gathers was PSBinStack (ProGold®), which calculates conversion points according to RMS velocity function for converted waves, γ_0 (vertical Vp/Vs ratio) and γ_2 (RMS Vp/Vs ratio). The conversion point is given by (Thomsen, 1999):

$$x_c(x,t_{c0}) \approx x\left[c_0 + c_2\frac{\left(\frac{x}{t_{c0}V_{c2}}\right)^2}{\left(1+c_3\left(\frac{x}{t_{c0}V_{c2}}\right)^2\right)}\right]. \quad (1)$$

$x_c(x,t_{c0})$ is the conversion point as function of time and source-receiver offset,

$$c_0 = \lim_{x\to 0}\frac{x_c}{x} = \frac{\gamma_{eff}}{1+\gamma_{eff}},$$

$$c_2 = \frac{\gamma_{eff}}{2\gamma_0}\frac{(\gamma_{eff}\gamma_0 - 1)(1+\gamma_0)}{(1+\gamma_{eff})^3},$$

$c_3 = c_2/(1-c_0)$ and,

$$\gamma_{eff} = \gamma_2^{\,2}/\gamma_0 .$$

Slight variation in Vp/Vs ratio change significantly the conversion point and consequently, the final stacked image produced. Therefore, the CCP velocity analysis followed by stacking depends very much on previous knowledge of Vp/Vs ratio for the area. This information might be obtained by either well log information or extracted from the seismic data.

The low signal to noise ratio of Serra's data did not allow a good Vp/Vs ratio estimation. Moreover, the dipole sonic data available is from a very distant well. On the other hand, good estimations could be done on the Gulf of Mexico line also processed during this project. Besides, well log information for this specific line was very reliable.

As mentioned before, the CCP stacking technique is much dependent on the knowledge of the area. Several CCP binning and stack were produced using different values of Vp/Vs as input. However, the final images presented poor definition. One may conclude that this technique requires a specific design to provide sufficient CCP fold and, consequently, good illumination (Silva *et al*, 2003a).

Migration

Alternatively to CCP conventional technique, it was used the pre-stack time migration algorithm for converted wave. The aim was to get over the difficulties of NMO/CCP stack method. The algorithm used is called Kirc3DtimeCMig (ProGold®) and the input parameters are combination of P-wave RMS velocity and γ function.

The conversion points are calculated as follows (Schneider, 2002):

$$x = \frac{12h^2\left(\gamma^2+1\right) - C\left[2\cos\left(\frac{\phi}{3}+\frac{2\pi k}{3}\right)+1\right]}{12h\left(\gamma^2-1\right)}, \quad (2)$$

where $C = V_p^2T^2 + 4h^2\left(\gamma^2+1\right)$,

$$\phi = \cos^{-1}\left\{\frac{C^3 864 h^4 \gamma^2 V_p^2 t^2}{C^3}\right\}$$ and, h=offset.

The search for γ_2, or RMS Vp/Vs ratio, is also dependent on the data. The Serra dataset presented more difficulties to estimate γ_2 than the GOM dataset. After the measurement of Vp/Vs RMS (γ_2), the converted wave time section was adjusted to the P-wave time.

The final converted wave section did not show as good quality as the final summed (vertical geophone + hydrophone) P-wave section. However, compared to P-wave section for vertical geophone only, it can be noticed a similar image quality.

Results

The final P-wave section was built by summing vertical geophone and hydrophone components (Silva *et al*, 2003b). The vertical geophone section as well as the hydrophone section corresponds to single (geophone or hydrophone) component P-wave data. The converted wave section corresponds to the radial geophone data without any correction since the receivers were oriented along the OBC cable under tension. No coherent image at transversal geophone was expected since the lines are 2D and no major anisotropic features were expected at this location.

The final P-wave CMP stacked section was obtained by dual sensor summing the P-wave wave-field. Free-surface peg-legs were removed by this process (Fig.5) enhancing the P-wave section if we compare to the single component CMP stack (Fig. 6 or Fig. 7).

The final pre-stack migrated PS section shows continuous geological events, with good image quality. However, because of the shallow geology, part of the section is blurred (Fig. 8). However, the same effect is observed at vertical geophone final section (Fig. 7). This fact is due to erosional features of the shallow carbonate sequences of the Jandaíra formation, changing the data quality because of its degeneration in this part of the section. The migrated section for transversal component didn't show coherent signal, which indicates weak anisotropy in the area.

Conclusions

This paper shows multi-component processing of 2D/4C seismic data from Serra field.

The CCP stack image is extremely dependent of the conversion point, Vp/Vs ratio definition and converted waves algorithms.

The pre-stack time migration algorithm for converted wave was, therefore, the best alternative to build final PS image section on Serra data.

The dual sensor summed P-wave section presented improvements over the one component P-wave section The improvements were observed even though the water depth is very small. This fact suggests that dual sensor can be used for improving images even in shallow water or transition zone.

Acknowledgments

We would like to thank Petrobras/PRAVAP19 for the financial support. We thank UN RN-CE group, in special to Dr. Carlos Alberto Poletto for encouraging this project. Thanks are extended to Fairfied Industries Inc. for the technical support during the course of the project and to Dr. Carlos Rodriguez Suarez, Petrobras Un-Rio, for the many insights regarding the fundamentals of S-wave technology.

References

Harrison, M. P., 1992, *Processing of P-SV surface-seismic data: Anisotropy analysis, dip moveout and migration*: Ph. D. thesis, University of Calgary.

Hoffe, H. H., Cary, P. W. and Lines, L. R, 1999, A simple and robust method for combining dual-sensor OBC data? CREWES report.

Nahm, J. W., Duhon, M. P., 2003, "Interpretation and practical applications of 4C-3D seismic data, East Cameron gas fields, Gulf of Mexico"; *The Leading Edge*, 22, 300-309.

Neill, E.; Parker, L.; Shields, H.; Poletto, C. A.; Keller, O.; Fiori, J.; Campos, S.; Guimarães, M. A.; 2001, "Single and Multi-component seismic acquisition in shallow water and transition zone environments", 7CISBGf/TS25;

Schneider, W.A.J., 2002. "A simple, exact solution for the P-SV wave conversion point via prestack migration": *Geophysics*, 67, 1634-1636.

Silva, M. B. C., Guimarães, M. A. G., Windels, R., Leiderman, R., Artola, F. A. V., Fontoura, S. A, B., Fiori, J., 2003a, "Data decimation study for multi-component seismic acquisition purposes": SBGf 2003 Conference, abstract submitted.

Silva, M. B. C., Artola, F. A. V., Leiderman, R., Fontoura, S. A, B., 2003b, *Análise para parametrização de aquisição sísmica multicomponente, Relatório Final*, PRAVAP19, Internal Report GTEP-02/03

Stewart R. R., Gaiser, J. E., Brown, R. J., Lawton, D. C.; 2002, "Converted-wave seismic exploration: Methods", *Geophysics*, V. 67, 1348-1363;

Thomsen, L., 1999, "Converted-wave reflection seismology over inhomogeneous, anisotropic media": *Geophysics*, 64, 678-690.

Yilmaz, O., 1997, *Seismic Data Processing*, Investigations in Geophysics vol.2, SEG

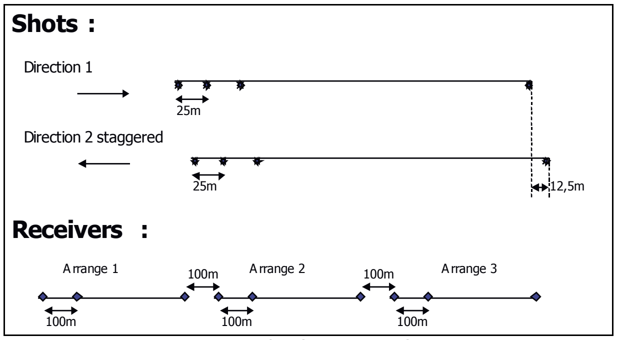

Figure 1 Acquisition design for Serra 2D/4C data

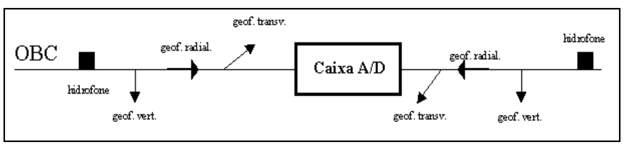

Figure 2: Disposição dos receptores 4C em relação à caixa A/D.

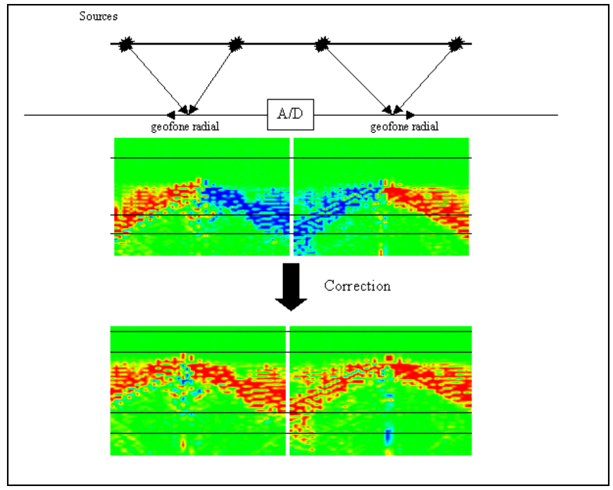

Figure 3: Result of polarity correction on radial component

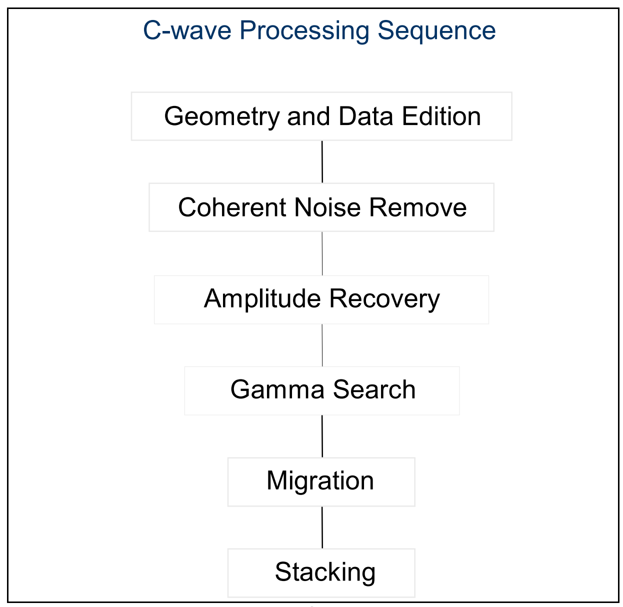

Figure 4: Processing sequence for converted wave data

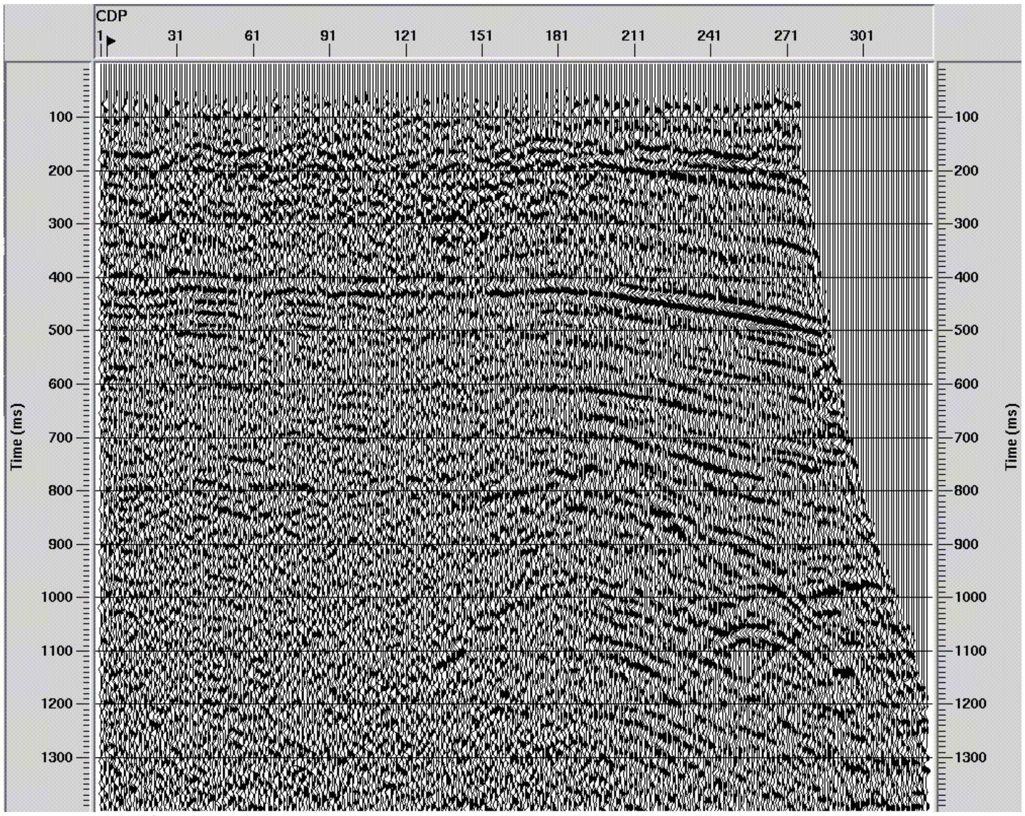

Figure 5: Final CMP P-wave image (applied dual sensor summing)

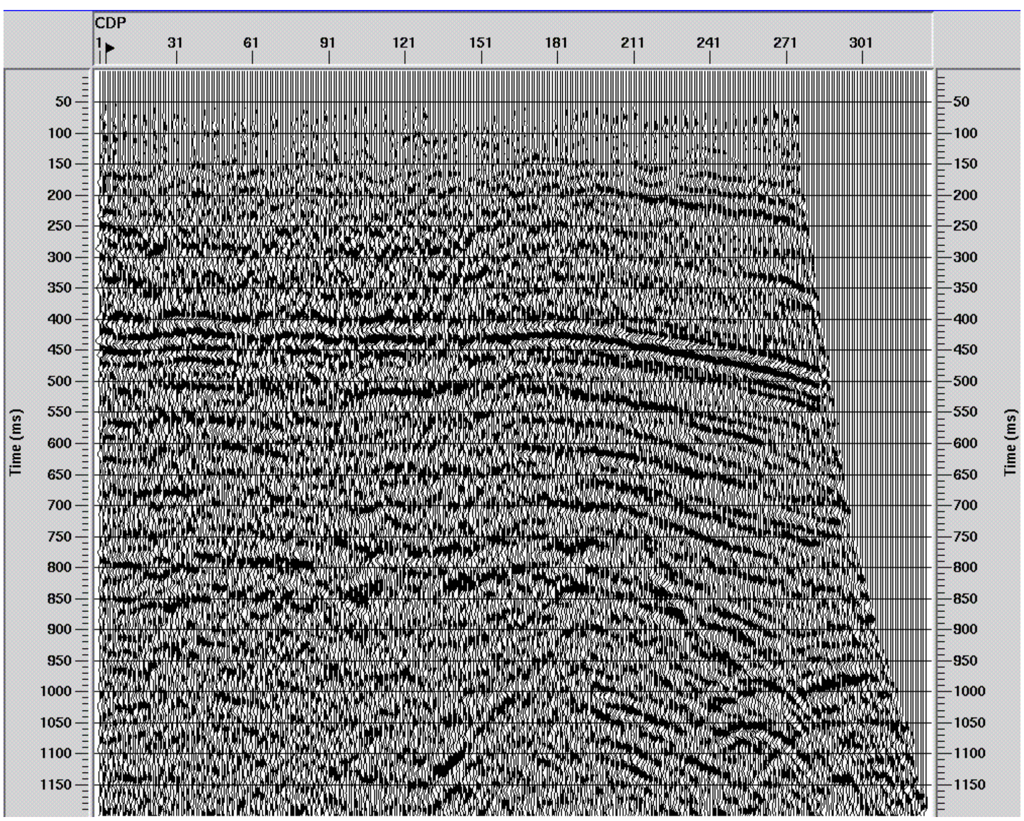

Figure 6: Final section for Hydrophone

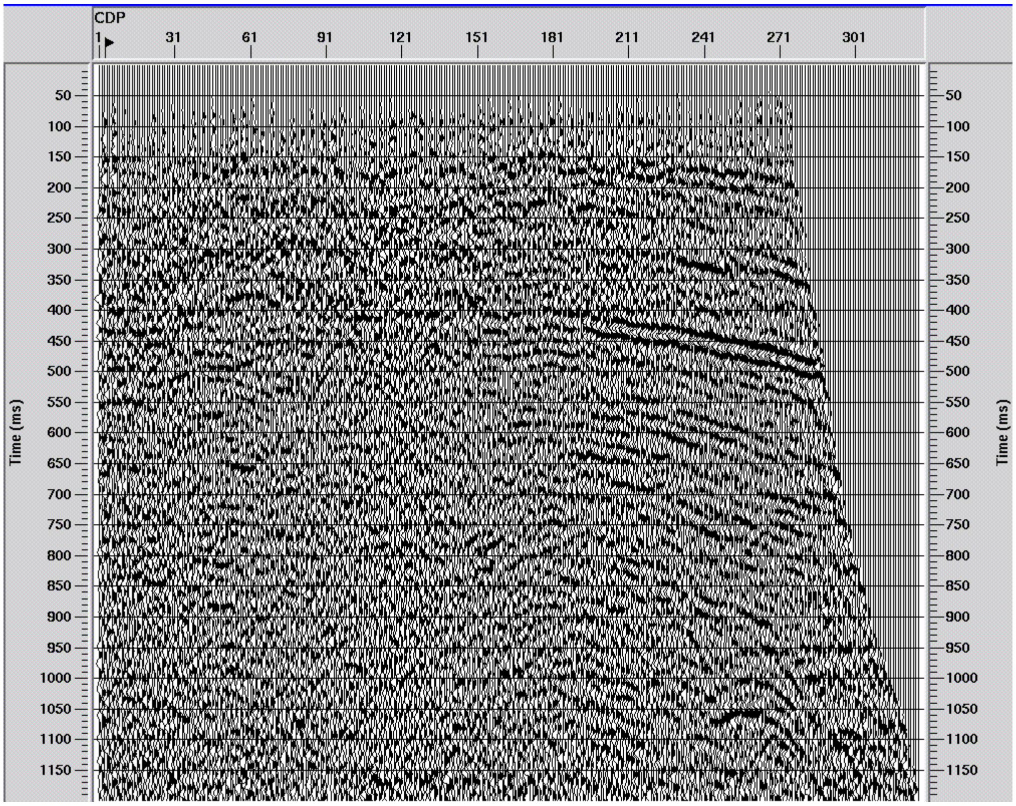

Figure 7: Final section for Vertical Geophone

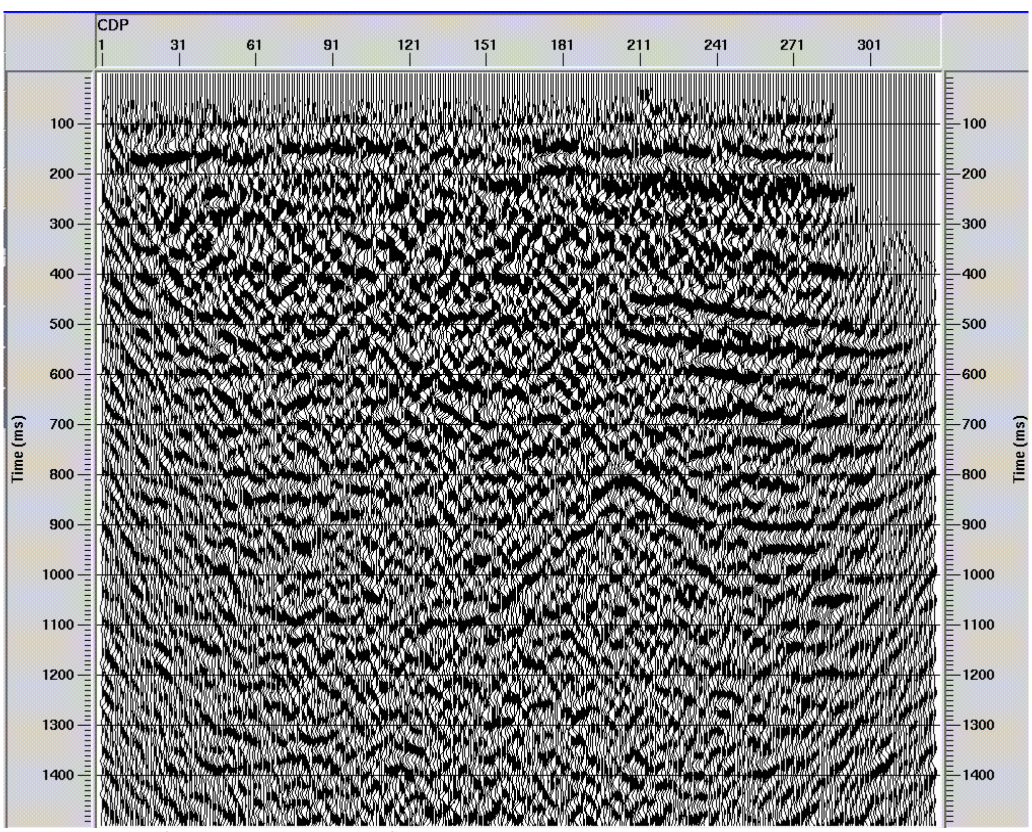

Figure 8: Final PS-wave section (Radial Geophone)